

# Structurally integrated transmitter beacon for underwater wireless optical communications in multiple ocean types

*Jonathan J.D. McKendry<sup>1</sup>, Xiaobin Sun<sup>2</sup>, Martin D. Dawson<sup>1</sup>, John Macarthur<sup>2</sup>, Henry Bookey<sup>2</sup>*

<sup>1</sup> Institute of Photonics, Department of Physics, University of Strathclyde, Glasgow, UK

<sup>2</sup> Fraunhofer Centre for Applied Photonics, Glasgow, UK

## ABSTRACT

In this paper we describe a structurally integrated optical transmitter beacon concept that consists of a side-scattering fiber that can conform to solid surfaces, such as the outer surface of a submersible Remotely Operated Vehicle (ROV), suitable for convenient deployment in underwater applications. By coupling a modulated optical signal from a laser diode into the fiber, an omnidirectional “beacon” is achieved. We demonstrate coarse Wavelength Division Multiplexing (WDM), illustrating that these beacons can transmit optical wireless data through several attenuation lengths in turbid water at aggregate data rates of up to 20 Mb/s.

**KEY WORDS:** Optical communications; wireless communications; underwater wireless.

## INTRODUCTION

With increasing demands on underwater information exchange, underwater communication technologies have gained more and more interest in underwater sensor networks, underwater mining, and aquatic rescue, amongst many others. Owing to the large bandwidth, low latency as well as small size, weight, power and cost (SWaP-C), light-emitting diodes (LEDs) / lasers (LDs)-based underwater wireless optical communication (UWOC) (Hanson and Radic, 2008) is becoming a complementary or even a competitive solution to its counterparts, e.g., acoustic (Song, Stojanovic and Chitre, 2019) and RF-based underwater communication (Palmeiro, Martín, Crowther, and Rhodes, 2011). With great efforts in maturing this technology, the physical layer verifications of UWOC systems are increasingly becoming comprehensive in both achievable transmission distances and speeds (Arvanitakis, Bian, McKendry, Cheng, Xie, He, Yang, Islim, Purwita, Gu, Haas, Dawson, 2020). By exploiting the low attenuation window of the water and single-photon-sensitive detection technologies such as Single-Photon Avalanche Diodes (SPADs), a UWOC system has been demonstrated with a transmission range up to 35.88 attenuation lengths (Hu, Mi, Zhou, and Chen, 2018). On the other side, Tsai, Lu, Wu, Tu, Huang, Xie, Huang, and Tsai (2020) has substantially multiplied the underwater channel capacity, having proved a 500-Gbps UWOC link using a five-wavelength polarization-multiplexing scheme.

Given the development mentioned above, it is an opportune time to consider the system’s robustness in real oceanic environments. Previous UWOC links are largely based on a point-to-point configuration, wherein the transmitter maintains continuous alignment with the receiver. However, complex and dynamic marine processes pose great challenges in maintaining the requirements of positioning, acquisition and tracking (PAT). These factors, including oceanic turbulence, turbidity, bubbles, link barriers, etc., result in severe performance degradation, such as beam scintillation, beam wandering, power fading, and bit transmission errors (Oubei, Shen, Kammoun, Zedini, Park, Sun, Liu, Kang, Ng, Alouini, and Ooi, 2018). Nevertheless, point-to-point links will be constrained with a small end coverage, limiting the mobility and quantity of receivers. Recently, several methods have been proposed to circumvent these issues. One of the solutions is diverging the transmission beam and leveraging the water scattering, forming a diffuse-line-of-sight (diffuse-LOS) link or even a non-line-of-sight (NLOS) link (Sun, Kong, Alkhazragi, Shen, Ooi, Zhang, Buttner, Ng, and Ooi, 2020). Alternatively, enlarging the photodetector’s sensitive area could also improve both practicality and connectivity between underwater signal transceivers (Kang, Trichili, Alkhazragi, Zhang, Subedi, Guo, Mitra, Shen, Roqan, Ng, Alouini, Ooi, 2019).

In this article, we reported our structurally integrated transmitter concept for alleviating the requirements on pointing in a UWOC link, and enhancing link’s robustness in the presence of challenging underwater channels. The transmitters were created by winding a length of Corning® Fibrance® side-scattering fiber around Perspex cylinders. Coupling blue (B)/green (G) laser light into these fibers creates cylindrical optical beacons that transmit light in an omnidirectional fashion. A photograph of this fiber beacon concept is shown in Fig. 1(a), where a green-emitting beacon is mounted onto the side of an ROV. In future, the side-scattering fibre could be directly integrated onto the chassis of underwater vehicles. The transmitter beacon thus shows a broadcasting capability, enabling omnidirectional communication. Using a Field-Programmable Gate Array (FPGA)-based On-Off Keying (OOK) modulation scheme, we demonstrated a 1.5 m, 20-Mbps G/B laser-based wavelength-division-multiplexing (WDM) wireless communication link with our transmitter beacon. The performance of the link has been tested in multiple artificially emulated ocean types. It was found that with increasing turbidity, the received power decreases. However, the G/B beacon could remain an effective communication link with a data rate of 10 Mbps/5 Mbps in the presence of 150 ml added antacid (a concentration of  $\approx$

0.093%). Optical modelling in Zemax OpticStudio® of the transmitter beacon has been further carried out. The simulation shows that the green beacon outperforms the blue beacon in a turbid underwater environment. With the green transmitter beacon, an effective 10-Mbps communication link over ~112 attenuation lengths remains. With that, we believe our structurally integrated transmitter beacon could play an active role in the internet-of-underwater-things (IoUT), acting as an underwater router for the underwater networks.

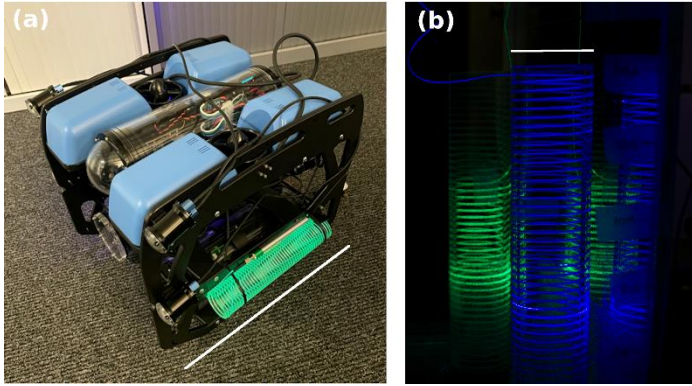


Fig. 1 (a) Green-emitting fiber beacon mounted onto an ROV and (b) blue and green-emitting beacons submerged in clear tap water. Scale bars represent 45 and 5 cm, respectively.

## EXPERIMENTAL SETUP

The experimental setup used here is shown in Fig. 2. A glass tank with dimensions 1.5 m length, 0.35 m width and 0.35 m height was filled with 160 l of clear tap water. Matt black plastic sheets were placed on the walls along the length of the tank and on its base, in order to reduce reflections from the walls of the tank.

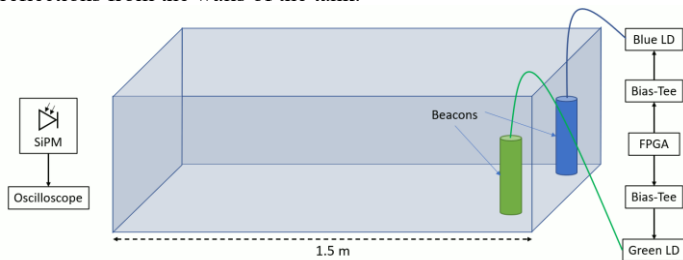


Fig. 2 Schematic illustration of fiber beacon optical communication experimental setup.

Fiber beacons were created by etching a spiral groove into the side of 25 cm high hollow and transparent Perspex cylinders, each with a diameter of approximately 5 cm. A length of Corning® Fibrance® side-scattering fiber was inserted into these grooves. Coupling light into these fibers creates cylindrical optical beacons that transmit light in an omnidirectional fashion, with approximately 5 mW of optical power transmitted per beacon. A photograph of the beacons submerged in clear tap water is shown in Fig. 1(b).

The two fiber beacons were submerged in the water and placed at one end of the tank. Light from blue and green laser diodes (LDs, peak wavelength of 450 and 520 nm, respectively) were coupled into respective fibers. Each LD was biased via a bias-tee and modulated using a 0 to 3.3 V On-Off Keying (OOK) signal generated by a Field-Programmable Gate Array (FPGA, Opal Kelly XEM3010). A different Pseudo-Random Bit Stream (PRBS) was applied to the two different LDs, each  $2^7-1$  bits long.

A receiver was placed outside of the tank, at a 1.5 m distance from the beacons. This receiver was a Silicon Photomultiplier (SiPM, SensL J Series 30035) with an active area  $3 \text{ mm} \times 3 \text{ mm}$ . This SiPM is in effect an array of Single Photon Avalanche Diodes (SPADs) with their outputs combined together to provide a quasi-analog output. A 1" diameter optical short pass filter (cut-on wavelength 500 nm) or long pass filter (cut-off 500 nm) was placed in front of the SiPM to select either the blue or green beacon, respectively, and to reject ambient light.

The modulated signals received by the SiPM were recorded using a 1 GHz bandwidth oscilloscope and saved for offline analysis. Water samples of varying turbidity were implemented by adding antacid to the tap water, a technique commonly reported elsewhere, in order to study the effect of increased turbidity on the Bit-Error Ratio (BER) of the received signals.

## Water Sample Characterization

As mentioned previously, the effect of increased attenuation of optical signals in natural waters was mimicked in the laboratory-based setting by adding antacid to clear tap water. Adding more antacid has the effect of increasing the absorption and scattering of light as it propagates through the water.

The attenuation coefficient as a function of the volume of added antacid was estimated as follows. Light from either the blue or green laser diode was collimated using a lens and directed to propagate through the 1.5 m length of the tank. The laser beam was then incident on an optical power meter sensor (ThorLabs S121C) to measure the transmitted power. Antacid was added to the tank, which contained 160 l of clear tap water, and mixed thoroughly to ensure it was homogeneously suspended in the water. The transmitted power through the new mixture was then measured. The attenuation coefficient for each volume of added antacid could then be estimated using Equation (1)

$$P_r(d) = P_t e^{-c(\lambda)d} \quad (1)$$

Where  $P_t$  and  $P_r$  are the transmitted and received powers, respectively,  $d$  is the distance the light propagates through the sample, and  $c(\lambda)$  is the attenuation coefficient at the wavelength of interest. The estimated attenuation coefficients measured at 450 and 520 nm as a function of added antacid is shown in Fig. 3.

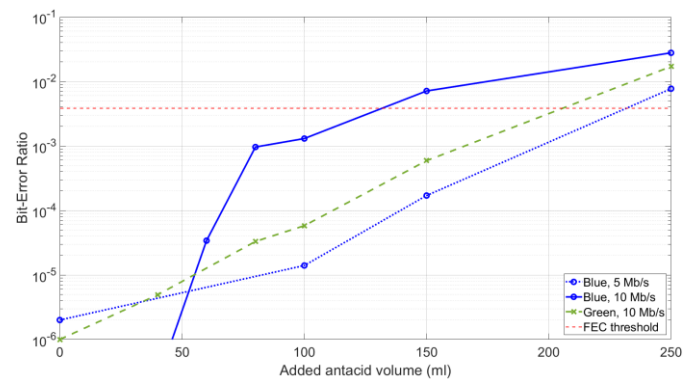


Fig. 3 Attenuation coefficients versus the volume of antacid added to 160 l of clear tap water. The red dashed and dotted lines represent the corresponding diffuse attenuation coefficients for Jerlov water types III and 9C, respectively.

Natural water types may be classified into Jerlov water types, where Jerlov water types I, II and III refer to oceanic water types of increasing

turbidity, and 1C to 9C referring to coastal water types, also of increasing turbidity. The diffuse attenuation coefficients, estimated at 450 nm for Jerlov types III and 9C are also shown in Fig. 3 for reference (Solonenko and Mobley 2015). It can be seen that above 10 ml the water samples used here were more turbid than even the most turbid Jerlov coastal water type. It can also be seen that at above 60 ml the attenuation coefficients appear to plateau. This may be attributed to the water conditions changing from a regime where single-scattering behavior dominates, and scattered photons are effectively “lost”, to one where received photons may undergo multiple scattering events.

Finally, we note that at the highest concentrations of antacid, optical signals propagating the 1.5 m length of the tank experience the equivalent of between 10 and 12 attenuation lengths, where one attenuation length is defined as the distance through a sample at which the received signal decreases to  $1/e$  of the transmitted value. The following section details the effect of these different water types on the BER.

## DATA TRANSMISSION RESULTS

The received signals recorded from the SiPM were analyzed in MATLAB® to estimate the corresponding Bit-Error Ratio (BER) for each. A methodology based on Shake and Takara (2002) was used to estimate the BER from the received signal as follows. The signal was sampled and the averaged Q-factor is calculated from these sampled values according to Equation (2).

$$Q = \frac{|\mu_1(t) - \mu_0(t)|}{\sigma_1(t) + \sigma_0(t)} \quad (2)$$

Where  $\mu$  and  $\sigma$  are the mean values and standard deviations of the sampled logic 1 and logic 0 levels, respectively. From Shake and Takara (2002) the Q-factor and BER are related according to Equation (3).

$$BER = \frac{1}{2} \operatorname{erfc} \left( \frac{Q}{\sqrt{2}} \right) \quad (3)$$

A BER lower than  $3.8 \times 10^{-3}$  can be considered “error-free” as below this value Forward Error Correction (FEC) codes with a modest (7%) overhead can be applied to the transmitted data, allowing errors to be detected and corrected (Islim et al. 2017). From this, the signals transmitted from both the blue and green fiber beacons were found to be error-free through 1.5 m of clear tap water when each was operating at an OOK data rate of 10 Mb/s.

Adding antacid to the tap water increased the attenuation of the transmitted optical signal through scattering and absorption. This reduces the signal-to-noise ratio (SNR) at the receiver, degrading the received signal and causing more bit-errors. This is demonstrated visually in Fig. 4 which shows photographs of the blue and green fiber beacons as viewed through 1.5 m of clear tap water and tap water with added antacid. The cloudy effect that the antacid has on the water and the propagation of the optical signals can clearly be seen in Fig. 4(b).



Fig. 4 photographs of fiber beacons viewed through 1.5m of (a) clear tap

water and (b) tap water mixed with antacid.

The effect this has on the BER is shown in Fig. 5. With an increasing addition of antacid the BER for all data rates and both beacons increases. It can be seen in Fig. 5 that when 150 ml of antacid is added to 160 l of clear tap water (corresponding to a concentration of  $\approx 0.094\%$ ) that error-free data transmission was obtained over the 1.5 m distance at data rates of 10 and 5 Mb/s for the green and blue beacons, respectively, giving an aggregate data rate of 15 Mb/s. This corresponding attenuation coefficient at this concentration is  $\geq 7.5$  and  $6.8 \text{ m}^{-1}$  for blue and green, respectively, meaning that this data was transmitted over  $>10$  attenuation lengths. The lower achievable data rate from the blue beacon at this concentration, and the lower performance of the blue beacon in general, may be attributed to a poorer coupling of laser light into the Fibrance® fiber, leading to a lower transmitted optical power from the beacon, which can be improved in future with improved coupling optics. It should also be noted that the optimal wavelength for optical transmission, where optical signals experience the least absorption and scattering, tends to shift to longer wavelengths as the water turbidity increases (Solonenko and Mobley 2015).

It can also be seen in Fig. 5 that both beacons were able to transmit error-free when 100 ml of antacid was added (a concentration of  $\approx 0.062\%$ ), for an aggregate data rate of 20 Mb/s.

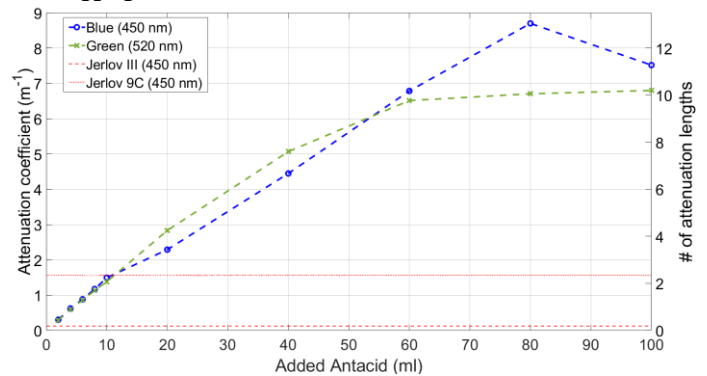


Fig. 5 BER versus concentration of antacid in tap water for the blue and green fiber beacons, as measured through 1.5 m of water.

## SIMULATION RESULTS

To explore the potential use of the structurally integrated transmitter beacon for long range communication links, beyond the physical distances that could be shown in our 1.5 m long tank, a performance envelope was determined using ray tracing simulations, performed using Zemax OpticStudio®. The transmitter was modeled as a filament. The simulation was setup to determine the communication capability of the transmitter beacon under different wavelength, water turbidity and transmission distance. Therefore, the simulation was conducted to obtain the received optical intensity under these different conditions. All the parameters for the transmitter and receiver have also been summarized in Table 1. The attenuation and scattering coefficients of different water types are taken from Solonenko and Mobley 2015.

Figure 6(a) shows the received power detected 1.5-m away from the transmitter beacon under different water types for both blue and green light. It was found that for the clear water, the received power for the blue transmitter is higher than the green transmitter, while for the turbid ones, i.e., coastal water, harbor I, harbor II, the green outperforms the blue. This could be explained by the transmission window red-shift due to the water turbidity variations (Mascarenhas, Keck, 2018).

Table 1 - General simulation and assumptions.

Parameter	Value
Data rate	10 Mbps RZ-OOK
Emitted power	5mW
# of rays traced	$1 \times 10^8$
Emission wavelength	450 nm/520 nm
Filament radius/Height/Turns	2.5mm/250mm/40
Receiver aperture	3 mm×3 mm
Photon detection efficiency	0.35@450 nm 0.25@520nm
Dark count rate	$4.5 \times 10^5$ Hz
# of pixels of receiver	5676
Probability of cross talk	0.08
Probability of after-pulsing	0.075
SiPM Deadtime	50 ns
Mean size of antiacid molecule	625 nm
Refractive index of antiacid molecule	1.559
Water types	Clear/Coastal/Harbor I / Harbor II/100 ml antiacid in 160 l water

With that, we further investigate the possible maximum achievable range using the green beacon in the turbid water. In this case study, we adopted a much more turbid water for emulating an extreme case, i.e., 100 ml antiacid added in 160 L water ( $\sim 7.5 \text{ m}^{-1}$  attenuation coefficient). The results have been shown in Fig. 6(b). It was found that a data rate of 10 Mbps over a transmission distance of 15 m ( $\sim 112$  attenuation lengths) could still be achieved in such turbid water channel.

## CONCLUSIONS

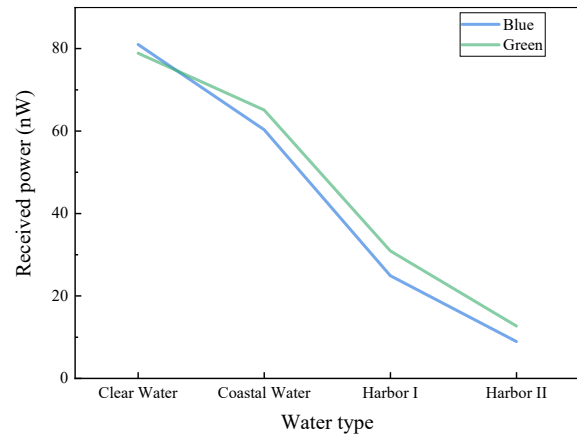
In this paper we have presented a low SWaP-C omnidirectional Underwater Optical Wireless Communication “beacon” concept, comprising of side-scattering fibres and modulated laser diodes. Using a single-photon sensitive “Silicon Photomultiplier” receiver and simple On-Off Keying modulation, wireless data transmission at up to 20 Mb/s over 1.5 m of water was demonstrated using blue and green-emitting beacons. This was possible even when antiacid was added to the water to increase turbidity, with this optical link being maintained even over approximately 10 attenuation lengths.

Using computer simulations to model what could be achieved outside of our test tank, we found that 10 Mb/s per beacon should be possible through turbid water at distances of up to 15 m.

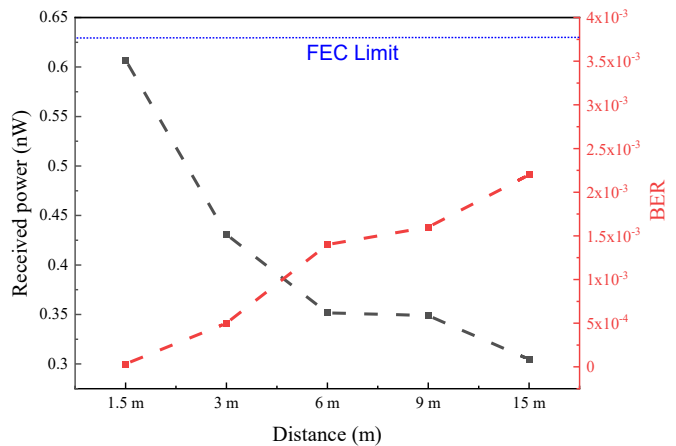
In future these side-scattering fibers could be integrated directly onto the chassis of underwater vehicles to further reduce the size and weight of the transmitter. Data rates could be increased further by adding additional transmitter wavelengths for enhanced Wavelength Division Multiplexing (WDM), or by using more advanced modulation schemes. Transmission distances could be increased by optimizing the output power of the laser sources, or reducing the coupling losses from the laser into the fibers.

## ACKNOWLEDGEMENTS

We acknowledge Dr. Johannes Herrnsdorf for the use of his FPGA interface. Supporting data can be found at <https://doi.org/10.15129/e24e4452-fb5a-4608-a8d9-3de4d401f239>



(a)



(b)

Fig. 6 (a) received power for the green and blue beacon under different water turbidities with a transmission distance of 1.5 m, (b) received power and BER for a green beacon-based 10-Mbps link over different transmission distances.

## REFERENCES

- Arvanitakis, G-N, Bian, R, McKendry, J-J, Cheng, C, Xie, E, He, X, Yang, G, Islim, M-S, Purwita, A-A, Gu, E, Haas, H, Dawson M-D (2020). “Gb/s underwater wireless optical communications using series-connected GaN micro-LED arrays,” *IEEE Photonics Journal*, 12(2), 7901210.
- Hanson, F. and Radic, S (2008). “High bandwidth underwater optical communication,” *Applied Optics*, 47(2), 277–283.
- Hu, S, Mi, L, Zhou, T, and Chen, W (2018). “35.88 attenuation lengths and 3.32 bits/photon underwater optical wireless communication based on photon-counting receiver with 256-PPM,” *Optics Express*, 26(17), 21685–21699.
- Islim, M, S, Ferreira, R, X., He, X, Xie, E, Videv, S, Viola, S, Watson, S, Bamiedakis, N, Penty, R, V., White, I, H., Kelly, A, E., Gu, E, Hass, H, Dawson, M, D. (2017). “Towards 10 Gb/s Orthogonal Frequency Division Multiplexing-Based Visible Light Communication Using a GaN Violet Micro-LED,” *Photonics Research* 5(2): A35-A43.
- Kang, C, Trichili, A, Alkhazragi, O, Zhang, H, Subedi, R, Guo, Y, Mitra, S, Shen, C, Roqan, I-S, Ng, T-K, Alouini, M-S, Ooi, B-S (2019). “Ultraviolet-to-blue color-converting scintillating-fibers

- photoreceiver for 375-nm laser-based underwater wireless optical communication,” *Optics Express*, 27(21), 30450-30461.
- Mascarenhas V., Keck T. 2018. "Marine Optics and Ocean Color Remote Sensing". In: Jungblut S., Liebich V., Bode M. (eds) *YOUMARES 8 – Oceans Across Boundaries: Learning from each other*. Springer, Cham. [https://doi.org/10.1007/978-3-319-93284-2\\_4](https://doi.org/10.1007/978-3-319-93284-2_4).
- Oubei, H-M, Shen, C, Kammoun, A, Zedini, E, Park, K, Sun, X, Liu, G, Kang, C-H, Ng, T-K, Alouini, M-S, and Ooi, B-S (2018). "Light based underwater wireless communications," *Japanese Journal of Applied Physics*, 57(8S2), 08PA06.
- Palmeiro, A, Martín, M, Crowther, I, and Rhodes, M (2011). "Underwater radio frequency communications," *Proc Oceans, Santander, IEEE*, 1–8.
- Shake, Ippei, and Hidehiko Takara (2002). "Averaged Q-Factor Method Using Amplitude Histogram Evaluation for Transparent Monitoring of Optical Signal-to-Noise Ratio Degradation in Optical Transmission System." *Journal of Lightwave Technology* 20(8), 1367–73.
- Solonenko, Michael G., and Curtis D. Mobley. 2015. "Inherent Optical Properties of Jerlov Water Types." *Applied Optics* 54(17): 5392–5401.
- Song, A, Stojanovic, M, and Chitre, M (2019). "Editorial underwater acoustic communications: Where we stand and what is next?" *IEEE Journal of Oceanic Engineering*, 44(1), 1–6.
- Sun, X, Kong, M, Alkhazragi, O, Shen, C, Ooi, E-N, Zhang, X, Buttner, U, Ng, T-K, and Ooi, B-S (2020). "Non-line-of-sight methodology for high-speed wireless optical communication in highly turbid water," *Optics Communications*, 461, 125264.
- Tsai, W-S, Lu, H-H, Wu, H-W, Tu, S-C, Huang Y-C, Xie J-Y, Huang, Q-P, Tsai, S-E (2020). "500 Gb/s PAM4 FSO-UWOC Convergent System With a R/G/B Five-Wavelength Polarization-Multiplexing Scheme," *IEEE Access*, 8, 2169-3536.